Distinct Functions of Activated Protein C Differentially Attenuate Acute Kidney Injury

Akanksha Gupta,* Bruce Gerlitz,* Mark A. Richardson,* Christopher Bull,† David T. Berg,* Samreen Syed,‡ Elizabeth J. Galbreath,‡ Barbara A. Swanson,§ Bryan E. Jones,* and Brian W. Grinnell*

*Biotechnology Discovery Research, †Integrative Biology, and ‡Pathology, Lilly Research Laboratories, Indianapolis, Indiana; and §Applied Molecular Evolution, San Diego, California

ABSTRACT

Administration of activated protein C (APC) protects from renal dysfunction, but the underlying mechanism is unknown. APC exerts both antithrombotic and cytoprotective properties, the latter via modulation of protease-activated receptor-1 (PAR-1) signaling. We generated APC variants to study the relative importance of the two functions of APC in a model of LPS-induced renal microvascular dysfunction. Compared with wild-type APC, the K193E variant exhibited impaired anticoagulant activity but retained the ability to mediate PAR-1-dependent signaling. In contrast, the L8W variant retained anticoagulant activity but lost its ability to modulate PAR-1. By administering wild-type APC or these mutants in a rat model of LPS-induced injury, we found that the PAR-1 agonism, but not the anticoagulant function of APC, reversed LPS-induced systemic hypotension. In contrast, both functions of APC played a role in reversing LPS-induced decreases in renal blood flow and volume, although the effects on PAR-1-dependent signaling were more potent. Regarding potential mechanisms for these findings, APC-mediated PAR-1 agonism suppressed LPS-induced increases in the vasoactive peptide adrenomedullin and infiltration of iNOS-positive leukocytes into renal tissue. However, the anticoagulant function of APC was responsible for suppressing LPS-induced stimulation of the proinflammatory mediators ACE-1, IL-6, and IL-18, perhaps accounting for its ability to modulate renal hemodynamics. Both variants reduced active caspase-3 and abrogated LPS-induced renal dysfunction and pathology. We conclude that although PAR-1 agonism is solely responsible for APC-mediated improvement in systemic hemodynamics, both functions of APC play distinct roles in attenuating the response to injury in the kidney.

J Am Soc Nephrol 20: 267–277, 2009. doi: 10.1681/ASN.2008030294

Acute kidney injury (AKI) leading to renal failure is a devastating disorder,[1] with a prevalence varying from 30 to 50% in the intensive care unit.[2] AKI during sepsis results in significant morbidity, and is an independent risk factor for mortality.[3,4] In patients with severe sepsis or shock, the reported incidence ranges from 23 to 51%[5–7] with mortality as high as 70% *versus* 45% among patients with AKI alone.[1,8]

The pathogenesis of AKI during sepsis involves hemodynamic alterations along with microvascular impairment.[4] Although many factors change during sepsis, suppression of the plasma serine protease, protein C (PC), has been shown to be predictive of early death in sepsis models,[9] and clinically has been associated with early death resulting from refractory shock and multiple organ failure in severe sepsis.[10] Moreover, low levels of PC have been

Received March 14, 2008. Accepted August 28, 2008.

Published online ahead of print. Publication date available at www.jasn.org.

Correspondence: Brian W. Grinnell, Biotechnology Discovery Research, Lilly Research Laboratories, Lilly Corporate Center, Indianapolis, IN 46285-0444. Phone: 317-276-2293; Fax: 317-277-2934; E-mail: bgrinnell@lilly.com

highly associated with renal dysfunction and pathology in models of AKI.[11] During vascular insult, PC becomes activated by the endothelial thrombin-thrombomodulin complex, and the activated protein C (APC) exhibits both antithrombotic and cytoprotective properties. We have previously demonstrated that APC administration protects from renal dysfunction during cecal ligation and puncture and after endotoxin challenge.[11,12] In addition, recombinant human APC [drotrecogin alfa (activated)] has been shown to reduce mortality in patients with severe sepsis at high risk of death.[13] Although the ability of APC to protect from organ injury *in vivo* is well documented,[11,14,15] the precise mechanism mediating the response has not been ascertained.

APC exerts anticoagulant properties via feedback inhibition of thrombin by cleavage of factors Va and VIIIa.[16] However, APC bound to the endothelial protein C receptor (EPCR) can also exhibit direct potent cytoprotective properties by cleaving protease-activated receptor-1 (PAR-1).[17] Various cell culture studies have demonstrated that the direct modulation of PAR-1 by APC results in cytoprotection by several mechanisms, including suppression of apoptosis,[18,19] leukocyte adhesion,[19,20] inflammatory activation,[21] and suppression of endothelial barrier disruption.[22,23] *In vivo*, the importance of the antithrombotic activity of APC is well established in model systems[24,25] and in humans.[26] However, the importance of PAR-1-mediated effects of APC also has been clearly defined in protection from ischemic brain injury[27] and in sepsis models.[28] Hence, there has been significant debate whether the *in vivo* efficacy of APC is attributed primarily to its anticoagulant (inhibition of thrombin generation) or cytoprotective (PAR-1-mediated) properties.[17,29]

The same active site of APC is responsible for inhibition of thrombin generation by the cleavage of factor Va and for PAR-1 agonism. Therefore, we sought to generate point mutations that would not affect catalytic activity, but would alter substrate recognition to distinguish the two functions. Using these variants, we examined the relative role of the two known functions of APC in a model of LPS-induced renal microvascular dysfunction.

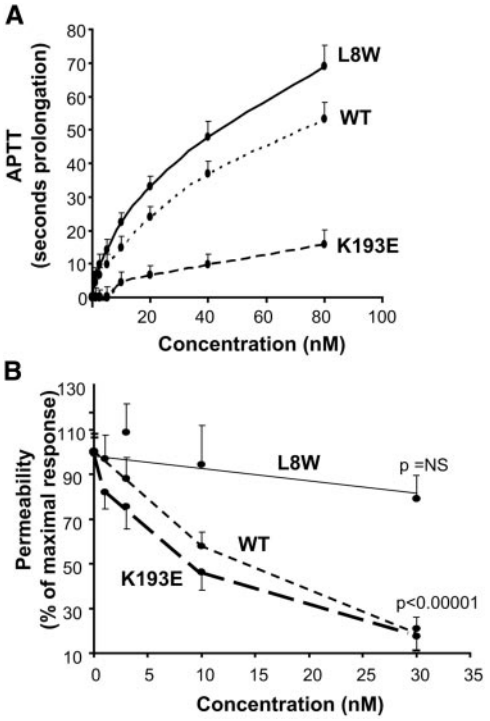

Figure 1. Determination of the antithrombotic and PAR-1-mediated properties of variants of APC. (A) Concentration dependence of wt-APC and variants L8W and K193E in a plasma APTT determination. Results are expressed as seconds of prolongation of the clotting time. Results are the mean ± SD, $n = 8$. (B) Effect of wt-APC, K193E, and L8W on permeability deficit in HUVECs by the Evans blue dye method described previously.[21] Results are mean ± SEM, $n = 4$.

RESULTS

Effect of Mutations on APC Anticoagulant and Cytoprotective Functions

Two variants of APC were generated by substitution of a Glu for Arg at position 193 in the protease domain of APC (K193E) and Typ for Leu at position 8 in the Gla domain (L8W). These mutations had no effect on synthetic substrates or plasma inhibitors at the active site (Supplemental Table 1 and 2). Because previous studies have shown that the simultaneous mutation of K191, K192, and K193 to Ala or Glu significantly reduced anticoagulant activity,[31,32] yet retained cell signaling,[32] we tested the effect of the single change of K193E on activated partial thromboplastin time (APTT). As shown in Figure 1A, K193E exhibited significantly less anticoagulant activity compared with wild-type APC (wt-APC). In repeated experiments, the concentration required to double the APTT by K193E was 20- to 30-fold higher than that of wt-APC. In contrast, the mutation L8W in the Gla domain retained the anticoagulant activity, actually being slightly more potent in this assay. Therefore, although the mutation of K193 had no effect on small substrate and serpin inhibitors, it appears to dramatically reduce interaction with APC's macromolecular substrates involved in coagulation inhibition.

Effect of Variants K193E and L8W on PAR-1-Dependent Cell Signaling

To assess the effect of these point mutations on the ability of APC to provide a cytoprotective signal via PAR-1, we determined their effect using a functional assay of endothelial permeability, previously shown to be PAR-1 dependent.[23] K193E dose-dependently suppressed PAR-1-dependent endothelial permeability, whereas L8W had no significant effect even at a maximally effective concentration of wt-APC (Figure 1B). In repeated experiments, the IC_{50} for K193E was significantly lower than wt-APC (5.6 ± 1.6 nM *versus* 10.3 ± 0.8 nM, $P < 0.05$, $n = 4$). In addition, K193E but not L8W induced calcium

flux in human umbilical vein endothelial cells (HUVECs) with a potency approximately twofold higher than wt-APC (Figure 2) and was PAR-1 and EPCR-dependent (Supplemental Figure 1). Wt-APC and K193E bound EPCR with equivalent affinity, whereas L8W did not significantly bind, suggesting that its lack of cytoprotective activity was due to defective EPCR interaction. (Supplemental Figure 2).

Effect of APC on Blood Pressure and Renal Blood Flow by Computed Tomography after LPS Challenge

We and others have previously shown that APC administered as a single bolus dose can ameliorate LPS-induced hypotension[30,33] and increase renal blood flow.[12] In rats, APC significantly blocked the LPS-induced reduction in mean arterial pressure (MAP) at doses of 30 and 100 μg/kg (Supplemental Figure 3). As previously shown in LPS models,[28] and as expected for the known anticoagulant activity, APC treatment blocked the fivefold rise in thrombin-antithrombin levels induced by LPS treatment (sham, 3.0 $\pm$ 0.9; LPS, 15.5 $\pm$ 6; APC, 2.8 $\pm$ 0.5ng/ml).

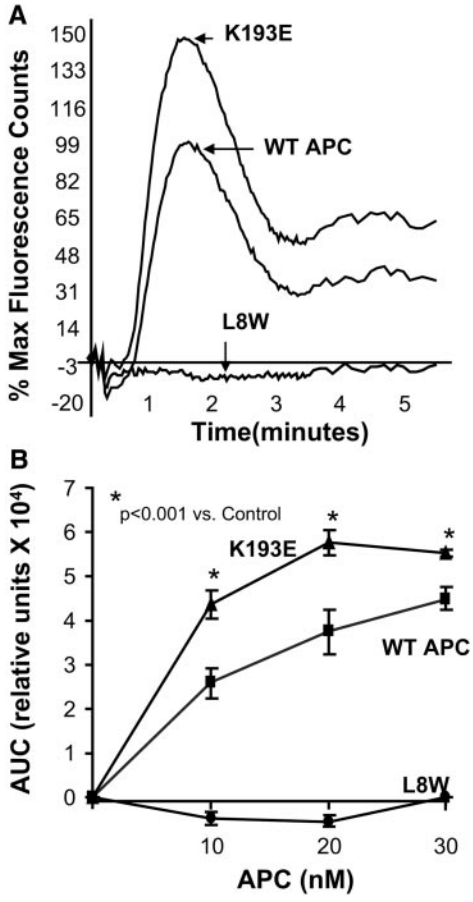

Figure 2. Determination of PAR-1-mediated properties of variants of APC by calcium flux and EPCR binding. (A) APC induces calcium flux in HUVEC. Wt-APC, K193E, and L8W were used at 80 nM in the presence of 1.0 U/ml hirudin. The wt-APC peak was normalized to 100%. (B) Determination of the calcium flux in HUVECs at varying concentrations of wt-APC and the variants. The area under the curve was determined using FLIPR software (v2.12, Molecular Devices, Sunnyvale, California). Results are mean $\pm$ SEM, $n = 8$.

Computed tomography (CT)-perfusion imaging was used to assess and quantify LPS-induced functional defects and the effect of APC treatment. As shown in the images in Figure 3A, administration of LPS significantly reduced renal blood flow, as demonstrated by the reduced intensity in the CT image. In repeated studies quantifying the CT analysis, renal blood flow and volume were reduced by approximately 43 and 39%, respectively, as compared with the sham group (Figure 3, B and C). However, after treatment with APC (100 μg/kg bolus), we observed a complete restoration in renal blood flow and volume. Although the lower dose of APC (30 μg/kg) resulted in suppression in the reduction in MAP (Supplemental Figure 3), there was no improvement in the renal blood flow and volume at this dose. As previously reported[12] and described in the supplemental data, the effect of APC on renal blood flow was independent of its effect on MAP.

Effect of PAR-1 Signaling Variant on Vascular Parameters during LPS Challenge

The role of APC in mediating anti-inflammatory properties via PAR-1 signaling is well documented in cell culture systems. However, the physiologic relevance of PAR-1 cleavage by APC *in vivo* has been controversial.[28,29,34] To address this issue, we examined the effect of K193E on modulating LPS-induced hypotension and renal blood flow. As shown in Figure 4A, administration of K193E at 30 μg/kg in LPS-treated rats significantly reversed the decrease in MAP after LPS treatment. Analysis of both renal blood flow and volume by CT perfusion analysis revealed that K193E at this dose also blocked the effect of LPS (Figure 4, B through D), although as was shown in Figure 3, the higher dose of wt-APC was required for this effect. These data are consistent with the *in vitro* data showing that K193E is more potent at PAR-1 signaling (Figures 1B and 2). APC-mediated PAR-1 agonism *in vivo* was confirmed by measuring phospho-ERK1/2 in the kidney (Supplemental Figure 4). Taken together, these data conclusively demonstrate that amelioration of LPS-induced hypotension is indeed mechanistically coupled to APC signaling via PAR-1. Moreover, PAR-1 signaling by APC is sufficient to improve renal blood flow and volume in this model.

Effect of Anticoagulant, but PAR-1-Inactive APC Variant, on Endotoxemia

To explore the role of APC's anticoagulant activity in mediating beneficial responses in the LPS model, we tested the effect of L8W on LPS-induced hypotension and renal function. At doses of 30 μg/kg, at which wt-APC was effective in suppressing the hypotensive response to LPS, L8W was ineffective (Figure 5A). Even at a higher dose of 100 μg/kg there was no protection from the LPS-induced reduction in MAP. Like wt-APC above, L8W effectively reduced thrombin-antithrombin levels to control (2.6 $\pm$ 0.5 ng/ml), whereas K193E showed no sig-

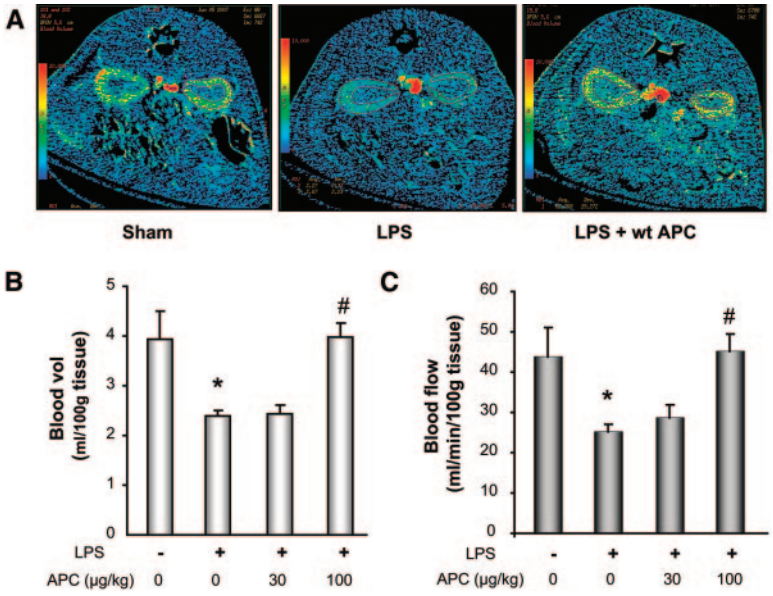

Figure 3. Effect of APC on renal hemodynamics by CT analysis in the rat endotoxin model. (A) Representative image of renal blood flow in control, LPS, and LPS + APC. (B) Quantification of CT for blood volume. (C) Blood flow after LPS and LPS + APC (30 and 100 μg/kg) administration. Data are represented as mean ± SEM, $n = 6$ per data group. $^{*}P \leq 0.05$ as compared with sham, $^{\#}P \leq 0.05$ as compared with respective LPS-treated group.

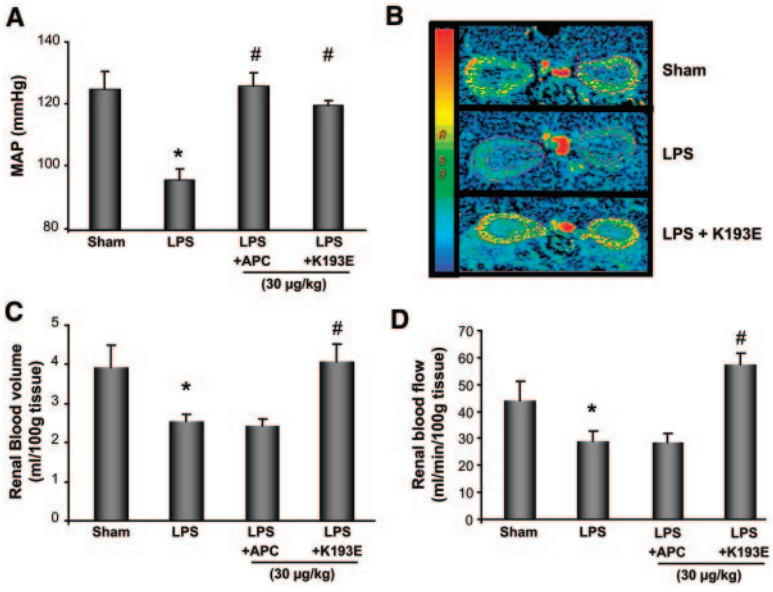

Figure 4. K193E effect on MAP and renal blood flow during endotoxemia. (A) Effect of APC (30 μg/kg) and K193E (30 μg/kg) on MAP. (B) Representative CT images depicting renal blood flow after APC and K193E treatment 3 h post-LPS administration. (C) Effect of APC (30 μg/kg) and K193E (30 μg/kg) on renal blood volume. (D) Renal blood flow in endotoxemic rats 3 h post-LPS administration. Data are mean ± SEM, $n = 6$ per group. $^{*}P \leq 0.05$ as compared with sham, $^{\#}P \leq 0.05$ as compared with respective LPS-treated group.

nificant difference from LPS-treated (16.8 ± 4.7 ng/ml) group. Thus, the anticoagulant activity of APC appears to have no role in the protection from hypotension.

We next assessed the effect of L8W on renal blood flow and volume. Although the dose of 30 μg/kg had no effect, unlike that observed with K193E, at a higher L8W dose of 100 μg/kg there was a significant improvement in both renal blood flow and volume (Figure 5, B and C). These results suggest that the anticoagulant activity of APC at higher doses can contribute to improvement of LPS-induced renal injury, but cannot aid in restoration of the systemic hemodynamics.

Effect of APC Variants on Renal Function and Pathology

We determined whether protection against renal injury observed at 3 h translated to improvement in renal function at 24 h post-LPS. LPS induced a significant renal insufficiency as denoted by increase in plasma blood urea nitrogen (BUN; Figure 6A). As observed at 3 h, wt-APC and K193E suppressed the LPS-induced increase in BUN, whereas a higher dose of L8W was required for significant effect. LPS induced significant multifocal nonthrombotic microangiopathy and early tubular damage (Figure 6B, low magnification Supplemental Figure 5). Similar to the effect on BUN, treatment with APC and K193E significantly reduced pathology at the 100-μg/kg dose, whereas a higher dose of L8W was required.

Renal Inductible Nitric Oxide Synthase Staining, Leukocyte Margination, and Plasma Adrenomedullin Levels

Because both variants could improve renal function, we sought to explore possible mechanisms. Previous studies have shown that APC can modulate hypotension and blood flow by suppressing inductible nitric oxide synthase (iNOS) and adrenomedullin (ADM) activation.[12,30,33] To assess the relative contribution of the two intrinsic activities of the molecule in driving both the improvement in systemic hemodynamics and in the renal vasculature, we examined the effect of L8W and K193E on plasma ADM levels. As shown in Figure 7A, at 3 h post-LPS treatment we observed a significantly elevated plasma level of the hypotensive peptide ADM compared with sham, which was largely suppressed by treatment of animals with wt-APC and K193E, but not L8W. With wt-APC, we previously showed that this effect was accompanied by a suppression in iNOS expression and iNOS-positive leukocyte infiltration.[30] By immunohistochemical staining, we observed weak expression of iNOS in kidney tissues from the sham animals, but intense iNOS staining and endothelial margination of iNOS-positive cells in the LPS-treated animals, indicating an activated nitric oxide pathway and vascular inflam-

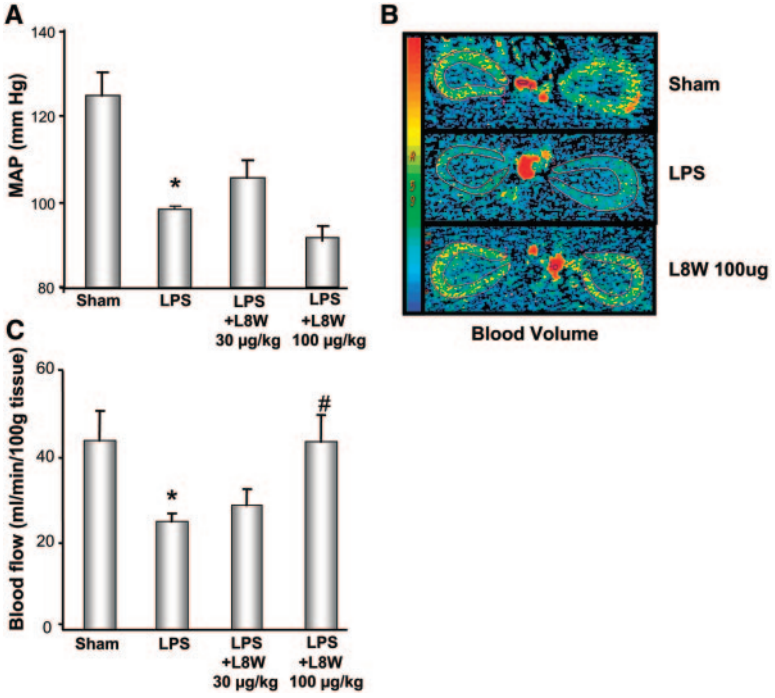

Figure 5. Effect of L8W on MAP and renal blood flow during endotoxemia. (A) Determination of MAP in the presence of L8W (30 and 100 μg/kg). (B) Representative CT images depicting renal blood volume after L8W treatment 3 h post-LPS administration. (C) Renal blood flow in the presence of L8W (30 and 100 μg/kg). Data are represented as mean ± SEM, $n = 6$ per data group. $^{*}P \leq 0.05$ as compared with sham, $^{\#}P \leq 0.05$ as compared with respective LPS-treated group.

mation (Figure 7B). K193E markedly reduced iNOS staining and endothelial margination, with the response being more dramatic than observed even for wt-APC. Similar to the effect on blood pressure (BP) and ADM, L8W had no effect on iNOS expression in the kidney tissue. These data suggest that the signaling component of the APC molecule is important in driving the improvement in vascular tone via suppression of vasoactive mediators such as ADM and iNOS. In addition, the suppression of leukocyte margination by APC is largely mediated by its PAR-1-dependent activity (K193E) and not its ability to suppress thrombin (L8W). The previously reported PAR-1 dependence of ADM regulation in cultured cells supports this observation.[30]

Modulation of Thrombin-Mediated Renal Markers of Inflammation by K193E and L8W

As shown above, L8W at higher doses could improve renal blood flow. To further explore the potential role of thrombin inhibition via L8W, we examined other mediators known to play a role in renal microvascular function during endotoxemia, including IL-6 and thrombospondin-1 (TSP-1), which are both induced by PAR-1 induction by thrombin,[35–38] and IL-18. Activation of these mediators in AKI has been associated with modulation of renal vascular inflammation and tone.[39,40] As shown in Figure 8, A and B, both IL-6 and IL-18 levels were significantly induced at 3 h post-endotoxemia. Surprisingly, K193E, which ameliorated renal injury and had the most significant anti-inflammatory response in terms of leukocyte margination (Figure 8), had no significant effect on these two proinflammatory cytokines. In contrast, L8W significantly downregulated plasma IL-6 and IL-18 levels as compared with the LPS-treated group. L8W, but not K193E, significantly reduced the induction in renal TSP-1 (Figure 8C). APC also has been shown to suppress renal angiotensin converting enzyme-1 (ACE-1) and thus the proinflammatory and vasoresponse through angiotensin II in the kidney.[11,12] As shown in Figure 8D, the protective effect of APC via suppression of the induction of ACE-1 in renal injury appears to be via the ability

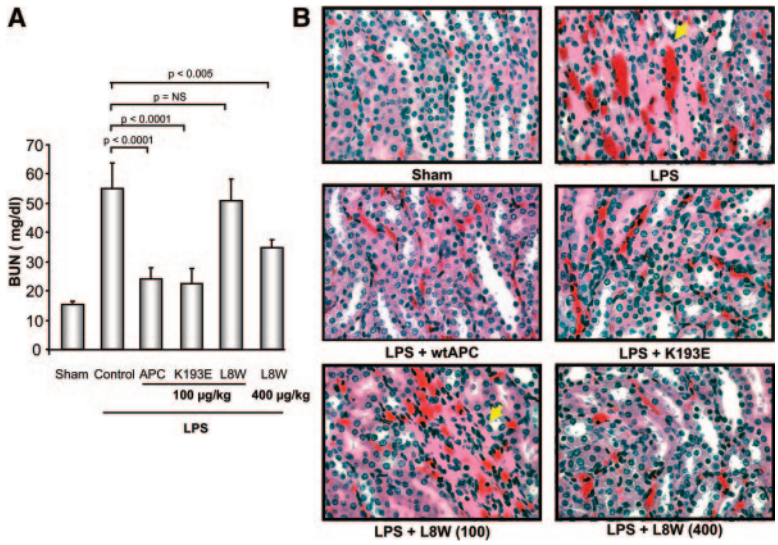

Figure 6. Effect of APC and variants on renal function and pathology. (A) Determination of plasma BUN levels 24 h post-LPS after treatment alone or after a single bolus dose of 100-μg/kg wt-APC, K193E, and L8W. Animals were also dosed at 400 μg/kg L8W. Data are represented as mean ± SEM, $n = 5$ per data group. (B) Representative hemotoxylin and eosin staining of kidney sections from sham and treated animals as in panel A. Notable pathology associated with the LPS treatment was diffuse multifocal ischemia with early tubular damage, characterized by nonthrombotic ischemic microangiopathy notable in the outer strip of the medulla (arrow), indicative of hypoxia as previously reviewed.[59,60] Supplemental Figure 5 shows lower magnification images. Consistent with the reduction in BUN levels, pathologic evidence of renal ischemia was significantly reduced by APC treatment and in the high-dose L8W animals and absent in the K193E animals.

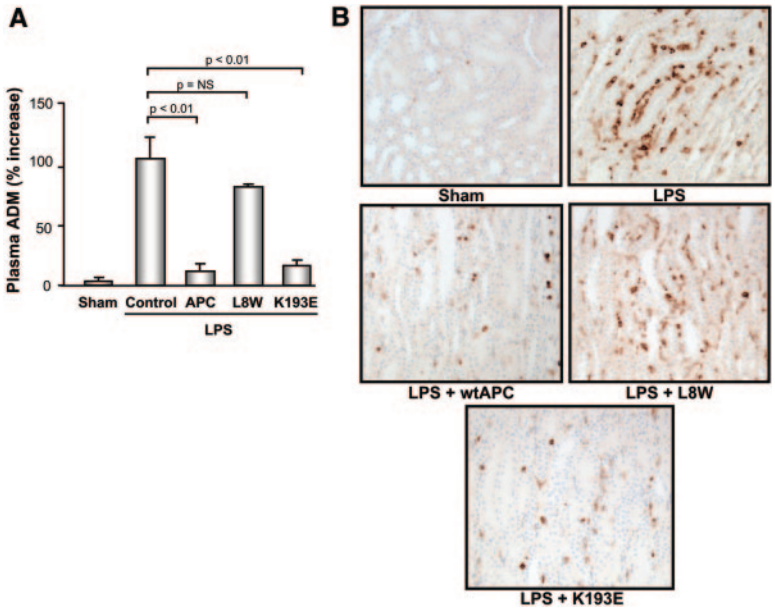

Figure 7. Effect of K193E and L8W treatment the vasoactive mediators ADM and iNOS. (A) Determination of plasma ADM levels after APC variant treatment. (B) Effect of APC variants on the degree of iNOS staining and leukocyte margination in kidney tissue obtained from sham and endotoxemic rats. $n = 6$ per data group.

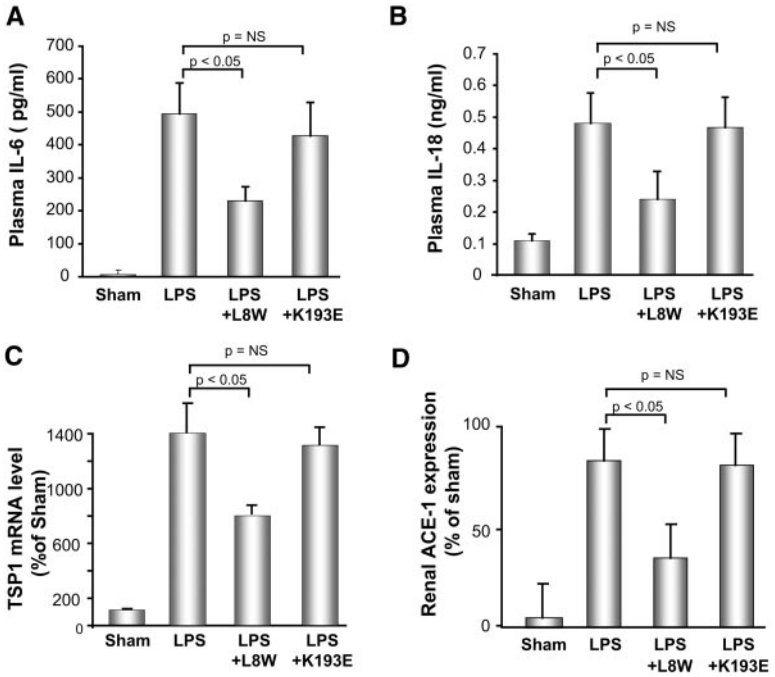

Figure 8. Effect of K193E and L8W treatment on the induction cytokines and on renal ACE-1 expression. Plasma level of (A) IL-6 and (B) IL-18 were determined by immunoassay. Data are represented as mean ± SEM, $n = 6$. (C) Relative expression of TSP-1 in the kidney after LPS treatment with and without APC variants. (D) Relative expression of ACE-1 in the kidney after LPS treatment with and without APC variants.

to inhibit thrombin generation and not the direct PAR-1-meditated signaling, because L8W but not K193E significantly suppressed its expression. These data demonstrate that both functions of APC can affect mediators previously associated with the protective effect of APC.

To provide additional support for the differential role of the variants, we examined caspase-3, which is induced by thrombin agonism[41–43] but blocked by APC agonism of PAR-1.[20] As shown in Figure 9, both L8W (by inhibiting thrombin generation and thus PAR-1 induction) and K193E (by direct agonism of PAR-1) suppress renal caspase-3 activation. As depicted in Figure 9B, APC appears to have complementary functions that at least in this model can independently result in the improvement in vascular function.

DISCUSSION

Various studies have demonstrated both anticoagulant and anti-inflammatory/cytoprotective properties of APC in model systems. Using the same active site, APC can cleave factors Va and VIIIa, resulting in the inhibition of thrombin,[16] and cleave and agonize PAR-1,[44] resulting in an anti-inflammatory/cytoprotective signaling response. Because thrombin itself is a proinflammatory mediator, there has been debate in the literature whether APC's effect on inflammation and vascular protection is mediated by inhibition of thrombin and its proinflammatory activity via PAR-1, or via the direct anti-inflammatory response by PAR-1 agonism. In this paper, using single point mutations that distinguish these two roles of APC, we provide evidence that both functions can contribute to a protective effect during organ injury.

LPS administration in rodents induces a hemodynamic response that results in alteration of renal blood flow and GFR, producing loss in renal function.[45] The pathogenesis of AKI secondary to endotoxin challenge has been attributed to impaired hemodynamics caused by systemic production of large amounts of nitric oxide and proinflammatory cytokines, along with enhanced renal vasoconstriction. In addition, leukocyte activation and microvascular dysfunction after kidney injury also play a key role in contributing to renal dysfunction.[46] Exogenous administration of APC has been shown to ameliorate renal dysfunction in animal models of endotoxemia and sepsis[11,12] as well as ischemia-reperfusion injury.[14] These effects have been attributed to suppression of the inflammatory response by inhibiting leukocyte-endothelial interactions and suppressing iNOS, ADM, and the cytokine response, resulting in

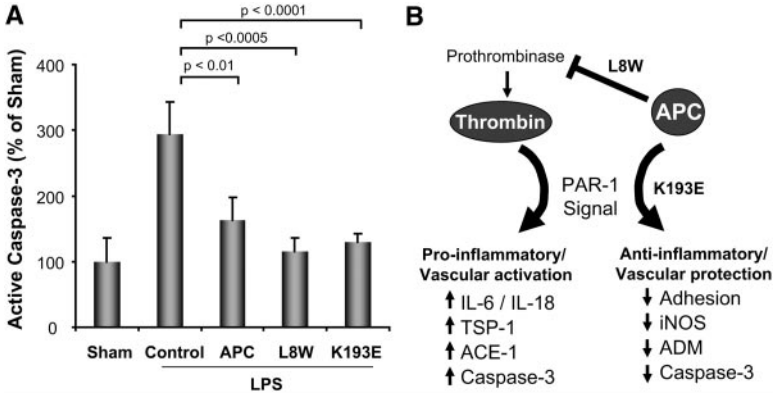

Figure 9. Effect of APC on caspase-3 activation and differential PAR-1 modulation. (A) Determination of degree of active caspase-3 in renal tissue and effect of APC and variant treatments (100 μg/kg). (B) Schematic of APC's distinct effects on PAR-1 agonism (K193E), and suppression of thrombin-mediated PAR-1 agonism by inhibition of thrombin generation (L8W). Redundant mechanisms appear to allow APC to improve vascular function because both variants improve renal blood flow and function by modulating distinct pathways.

an improvement in renal blood flow. In the study presented here, we observed that administration of a single bolus dose of APC blocked the hypotensive response to LPS and the associated iNOS and ADM induction and suppressed leukocyte infiltration into the kidney. These effects were clearly mediated via PAR-1 agonism because K193E, but not L8W, was protective. Thus, PAR-1 agonism alone was sufficient to inhibit LPS-induced renal vascular dysfunction.

The protection against BP drop, reduced renal blood flow, and rise in BUN conferred by K193E provide compelling evidence that PAR-1-mediated signaling is important. However, treatment with K193E did not alter common markers of inflammation, such as IL-6 and IL-18 levels, nor did it affect the level of renal ACE-1. In contrast, L8W markedly suppressed IL-6, IL-18, and renal ACE-1, all markers previously associated with renal dysfunction and protection with APC.[12] Of interest, thrombin is a potent inducer of IL-6 via activation of PAR-1,[35–37] suggesting that the effect of L8W is by reducing thrombin and thus thrombin-mediated PAR-1 activation. The lack of an effect of L8W on the hypotensive response is consistent with studies by Isobe *et al.* showing that inhibition of thrombin generation by active-site-inhibited factor Xa could not alter LPS-induced hypotension in an rat endotoxin model.[33] Moreover, studies with thrombin inhibition using heparin infusion in rats showed improved microvascular blood flow in the brain, which was independent of BP changes.[47]

A recent study by Kerschen *et al.*[28] has suggested that the antithrombin activity of APC is not important in the efficacy in murine models of sepsis. Furthermore, Taylor *et al.*[48] showed that active site-blocked factor Xa was unable to rescue animals from an endotoxin challenge despite preventing coagulopathy, and anticoagulants such as antithrombin and tissue factor pathway inhibitor failed to provide benefit in severe sepsis trials.[49,50] These data suggest that anticoagulation alone is not sufficient to provide protection in systemic microvascular dysfunction. However, our data would suggest that APC can have distinct effects on inflammatory activation and vascular function through the ability to block thrombin generation as well as to agonize PAR-1. Thus, the relative role of each function likely depends on the context and/or drivers of the particular vascular pathology, such as the degree of coagulopathy. Further studies will be needed to define the relative balance of these two activities in any particular disease context.

The surprising result of our study was that through very different pathways affecting vascular inflammation and tone, both functions of APC resulted in improvement in renal blood flow as a measure of kidney function postendotoxemia. As depicted in Figure 9B, the central player in the response to APC appears to be PAR-1, and whether APC directly agonizes the receptor to generate a protective response or blocks the proinflammatory activation of PAR-1 via thrombin, the net effect is an improvement in microvascular function. The results suggest that either the direct signaling response of APC (leading to effects such as reduced leukocyte infiltration, iNOS expression, and improved vascular tone) or the inhibition of thrombin and resulting suppression of pathways involving cytokine response and ACE-1 are independently sufficient to improve renal blood flow and volume, although the improvement in systemic hemodynamics is solely via PAR-1 agonism. Our data would suggest that both functions of APC may play independent, and possibly redundant roles depending on the disease context.

CONCISE METHODS

S-2366 Amidolytic Activity of APCs

The kinetics of hydrolysis of the tripeptide substrate Glu-Pro-Arg-*p*-nitroanilide (S-2366) were performed at 25°C in 150 mM NaCl, 20 mM Tris-HCl, 3 mM $CaCl_2$, 2 mg/ml BSA, pH 7.4 with recombinant APC (0.5 nM), with various concentrations of S-2366 (15.6 to 2000 μM). Reactions ($n = 6$) were carried out in 96-well microtiter plates (200 μl/well) and the absorbance at 405 nm was monitored in a ThermoMax kinetic microtiter plate reader. Kinetic constants were derived using SigmaPlot Enzyme Kinetics Module 1.1 (Michaelis-Menten Enzyme Kinetics nonlinear fit) software, a path length of 0.53 cm (Molecular Devices Technical Applications Bulletin 4-1), and an extinction coefficient for *p*-nitroaniline of 9620 $M^{-1} \cdot cm^{-1}$ at 405 nm as described previously.[51]

In Vitro Plasma Half-Life Determination

Inactivation of APCs and plasma half-lives were determined by incubating 20 nM APC in citrated plasma [human and rat, 90% (vol/vol)]

at 37°C. Aliquots were removed at selected times, and residual APC amidolytic activity was measured using the S-2366 chromogenic assay. Initial amidolytic activity reading (time = 0 min) was set as 100% and activity remaining at subsequent time points was calculated as a percentage of this initial activity. The half-life ($t_{1/2}$) was calculated by nonlinear regression analysis of the decay curves with SigmaPlot 8.0 (Enzyme Kinetics module) and the equation $t_{1/2} = \ln(2)/k1$ (app), where k1 (app) = the apparent first-order rate constant for inactivation.

APTT Assay

The anticoagulant activity of recombinant APCs (wild-type, L8W and K193E) was determined using an APTT assay as described previously.[52] In brief, the APCs were serially diluted in buffer consisting of 150 mM NaCl, 20 mM Tris-HCl pH 7.40, and 2 mg/ml BSA. APTTs were then determined by preincubating 20 μl of the APC dilution (or buffer alone, baseline control) with 50 μl of citrated plasma and 50 μl of APTT reagent (Helena Laboratories 5385) for 5 min at 37°C in a 96-well plate (CoStar 3596). Clotting reactions were then initiated by the addition of 50 μl of 25 mM $CaCl_2$ (prewarmed at 37°C), and absorbance at 595 nm was monitored using a ThermoMax plate reader (Molecular Devices) over a 5-min kinetic run with a 6-s read interval; clotting times were determined as "time to V_{max}" ($n = 8$). Assays were conducted using rat citrated plasma (Sprague Dawley, pooled from multiple animals) as well as human citrated reference plasma (S.A.R.P, Helena Laboratories 5185).

Cell Permeability Assay

Permeability was measured as the movement of Evans blue bound albumin across cell monolayers using a two-chamber system essentially as described previously.[23] In brief, the transformed human endothelial cell line EA.hy926 was maintained in a tissue culture incubator at 37°C and 5% CO_2; growth medium was DMEM/F-12 (3:1 ratio) supplemented with 10% FBS, 20 mM HEPES, and 50 μg/ml gentamicin. For permeability assays, EA.hy926 cells were trypsinized/seeded into HTS Transwell-24 plates (Corning CoStar 3399) at 20,000 cells/0.33 cm^2/well and grown to confluency over approximately 1 wk. Serum-free medium (SFM) was prepared by supplementing DMEM/F-12 medium (3:1 ratio) with 20 mM HEPES, 2 mg/ml BSA, 1× insulin-transferrin-selenium-X (Invitrogen 15630–080), and 50 μg/ml gentamicin. After visually confirming EA.hy926 monolayers using a microscope, the lower chamber medium was replaced with 600 μl SFM and the upper chamber medium was replaced with 100 μl of SFM containing 0 to 30 nM of the various recombinant APCs (wild-type, L8W or S3F). Plates were then incubated for 2 h at 37°C and 5% CO_2, after which the upper chamber medium was replaced with 100 μl SFM ± 5 nM human thrombin and the plate incubated 15 min at room temperature. Then 100 μl of DMEM/F-12 (3:1 ratio) containing 2% BSA and 0.6% Evans blue was added to the upper chambers and the plate was mixed briefly before incubating another 2 h at room temperature. The Transwell plate was then mixed again briefly and the upper chambers removed before transferring an aliquot from the lower chambers to a 96-well plate. This 96-well plate was then measured for absorbance at 650 nm using a ThermoMax plate reader (Molecular Devices).

Fluorometric Imaging Assay

HUVECs (Clonetics, Walkersville, Maryland) were seeded into a 96-well plate at 10^4 cells per well and incubated for 48 h at 37°C in 5% CO_2 until confluent. The monolayers were rinsed once with fluorometric imaging plate reader (FLIPR) buffer:HBSS (Invitrogen, Carlsbad, California) and 0.75% BSA fraction V (Invitrogen). The cells were labeled with 50 μl per well of 5 mM Fluor-4 am (Invitrogen) and 0.05% Pluronic F-68 (Life Technologies) in FLIPR buffer. The cells were incubated for 30 min at 37°C in 5% CO_2. After incubation the cells were washed three times with FLIPR buffer, and 50 μl of FLIPR buffer was added to each well. APC and APC mutants were diluted into FLIPR buffer with 1.0 U/ml hirudin (Calbiochem, San Diego, California) and added to 96-well polypropylene V-bottom plates (Greiner Bio-One, Germany). Calcium flux was measured in a FLIPR (Molecular Devices, Sunnyvale, California). For experiments with antibody treatment, we used anti-PAR-1 (ATAP2, sc-13503) or control normal mouse IgG (SC-2025, Santa Cruz Biotechnology, Santa Cruz, California), and anti-EPCR (purified rat anti-human CD201, #552500, BD Biosciences Pharmingen, San Jose, California) or control normal rat IgG (sc-2026, Santa Cruz Biotechnology). Antibodies were allowed to bind for 2 h at 37°C in 5% CO_2, then the plates were rinsed with FLIPR buffer and treated with APC and variants as above.

Determination of Binding to EPCR

EPCR binding by APC to EPCR-expressing cells was determined essentially as described previously.[53] HUVEC monolayers expressing high levels of EPCR, determined by FITC-labeled anti-EPCR antibody binding, were dissociated using enzyme-free dissociation buffer (Invitrogen). APC (81 nM) was mixed with the dissociated cells (1.5×10^5 cells/ml) on ice for 1h. The cells were then washed with HBSS/bovine albumin fraction V (Invitrogen) and bound again with the C1 anti-APC antibody (2 mg/ml) on ice for 2 h. The cells again were washed and labeled with goat anti-mouse IgG-PE on ice for 45 min and the amount of APC bound to the cells *versus* control IgG (no APC) was determined followed by flow cytometry.

To determine the kinetics of binding, Costar #3590 96-well EIA/RIA plates (Corning, Corning, New York) were coated with soluble human EPCR (obtained from Eli Lilly & Co.) at 50 μg/ml in carbonate-bicarbonate buffer #C-3041 (Sigma, St. Louis, Missouri). Control wells for nonspecific APC binding were coated with BSA fraction V (Life Technologies #15260, Invitrogen, Grand Island, New York) at 50 μg/ml. The plates were incubated overnight at 4°C, rinsed once with binding buffer (HBSS, Life Technologies #14025, Invitrogen, Grand Island, NY.; 10 mg/ml BSA fraction V, 20 mM HEPES buffer solution, Life Technologies 15630, Invitrogen, Grand Island, NY; 2 mM $CaCL_2$), and 200 μl/well binding buffer was added and incubated at room temperature for 1 h. After a rinse in binding buffer, varying concentrations of APC and the variants were added and the plates incubated for 2 h at room temperature. Plates were rinsed three times with binding buffer. Amidolytic activity of bound APC was determined by adding 175 μl/plate of 150 mM $NaCl_2$, 20 mM Tris pH 7.5, 3 mM $CaCl_2$, and 25 μl of a 1-mg/ml solution of S-2366 (Chromogenix, Lexington, Massachusetts) using a Molecular Devices SpectroMax 190 plate reader for a 1-h kinetic read at A_{405} to A_{595}, reading once every minute. K_d values were determined using SigmaPlot 8.0 software.

Animal and Surgical Procedure

Male Sprague-Dawley rats (Harlan, Indiana) weighing 250 to 300 g were used in the study. The rats were acclimatized to the laboratory conditions for at least 7 d after their arrival. Endotoxemia was induced by administration of *Escherichia coli* LPS (10 mg/kg, intravenous infusion for 30 min; LPS *E. coli* 111:B4, Sigma, Detroit, Michigan) using a tail vein catheter. The control group received pyrogen-free saline. In the APC-treated groups, recombinant human APC (100, 30, or 10 μg/kg, intravenous bolus) or the variants were administered before the administration of LPS in the respective groups. After 3-h post-LPS administration, renal blood flow and BP measurements were performed. BP was recorded using a tail-cuff system (CODA6). Animals were sacrificed at 3-h time points for collection of kidney tissue, and a blood sample was collected for analysis just before sacrifice. All experimental methods were approved by the institutional Animal Care and Use committee and were in accordance with the institutional guidelines for the care and use of laboratory animals.

To provide additional evidence of a sustained benefit, we also examined the effect of APC variants at 24 h after endotoxemia as described previously.[12] For 24-h studies, rats received an intraperitoneal injection of LPS (20 mg/kg). This concentration was based on a dose response that resulted in elevated BUN and no mortality at 24 h. APC and variants were administered at the time of induction of endotoxemia, and 24 h later the kidney and plasma were collected for histology and BUN analyses. BUN was determined using a Hitachi 911 clinical chemistry analyzer (Roche Diagnostics, Indianapolis, Indiana). For pathology, tissues were fixed, sectioned, and stained as described previously.[54] The slides were assessed for degree of pathology by a board-certified veterinary pathologist.

Functional CT and Quantification of Perfusion Parameters

Perfusion CT imaging was utilized to measure renal blood flow as described previously.[55–58] Briefly, animals were placed in the center of the CT scanner (Locus Ultra; GE Medical Systems, Milwaukee, Wisconsin) and a tail-vein catheter was inserted (BD Biosciences) for contrast agent injection. Single-location multisection (80 rows) cine CT scanning was begun 3 s before a bolus of 300 μl of iodinated contrast medium (150 mg/ml, Omnipaque; Amersham, Princeton, New Jersey) was administered via the tail vein at a rate of 3 ml/min. All images were acquired by using an 80-kVp tube voltage, an 60-mA tube current, and a 1-Hz rotation speed. The data obtained at functional CT were then reconstructed into a 153- by 153- by 403-μm voxel matrix with an improved temporal resolution of 0.5 s between images. The reconstructed image data were then transferred to an image workstation (Advantage Windows; GE Medical Systems) for calculating perfusion parameters. Absolute values of perfusion parameters—blood flow (in milliliters per minute per 100 g of rat tissue weight) and blood volume (in milliliters per 100 g)—were measured by using perfusion software (Perfusion II; GE Medical Systems). Using the highest spatial resolution pixel-by-pixel calculation technique created the parametric map images. To quantify functional CT parameters, we first used cursors to indicate a six-pixel region of interest within the aorta to determine the enhancement value of arterial input. A region of interest was then drawn on the raw CT images, on which the whole kidney was delineated by contrast enhancement. In addition to measuring the entire kidney, we marked as functional hot spots on the parametric images the areas inside the kidney where the highest blood flow and blood volume were measured.

Determination of Concentration of ADM, IL-6, and IL-18 in Rat Plasma, and ACE and TSP-1 mRNA in Kidney Tissue

Plasma ADM levels were measured using the kit supplied by Phoenix pharmaceuticals (Belmont, California) following the manufacturer's instructions as described previously.[30] Measurements of IL-6 and IL-18 were by immunoassay using the Rodent Multi-Analyte Profile (Rules Based Medicine; Austin, Texas). Renal ACE mRNA was measured using QuantiGene Plex (Panomics, Inc. Fremont, California) according to the manufacturer's recommendation. TSP-1 levels were determined from total RNA purified from kidneys with the RNeasy procedure (Qiagen) using a TaqMan gene expression assay for rat TSP-1 (# Rno1513693_m1, Applied Biosystems, Foster City, California).

Immunohistochemistry

Kidneys were fixed in 4% paraformaldehyde and embedded in paraffin. Five-micrometer sections were immunostained for iNOS using the automated Ventana Discovery XT staining module (Ventana Medical Systems, Tuscon, Arizona). The tissue was deparaffinized and antigen retrieval was performed using standard cell conditioning 1. The sections were incubated with rabbit anti-mouse iNOS (5 μg/ml, BD Transduction Labs) for 60 min followed by biotinylated goat anti-rabbit IgG (1:200, DAKO) for 20 min. Detection was performed using Ventana's DAPMap kit, and sections were taken offline for routine counterstaining with hematoxylin.

Active Caspase-3 Western Analysis

Protein lysates were prepared for Western analysis using the T-PER reagent (Pierce, Rockford, Illinois) containing complete protease inhibitor cocktail (Roche Diagnostics GmbH, Mannheim, Germany) from kidney tissues that had been preserved in RNA-later (Ambion Austin, Texas). The protein lysates were quantified by bicinchoninic assay (Pierce) and equal concentrations of each lysate were loaded for SDS PAGE and electroblotting. Cleaved caspase-3 was detected using the Apoptosis Marker:Cleaved Caspase-3 (Asp175) Western Detection Kit from Cell Signaling Technology, Inc. (Danvers, Massachusetts). The blots were stripped and reprobed using a monoclonal antibody to β-actin (Sigma) for normalization. Levels of cleaved caspase-3 and β-actin were quantified by analyzing the pixel density of each band from scanned autoradiograms using UnScanIt software (Silk Scientific Corporation, Orem, Utah).

Statistical Analysis

Data are presented as mean ± SEM. The biochemical data were analyzed by one-way ANOVA using JMP5.1 software (SAS Institute). After obtaining a significant F value, a *post hoc t* test was performed for inter- and intragroup comparisons. Statistical significance was realized at $P \leq 0.05$ to approve the null hypothesis for individual parameters.

ACKNOWLEDGMENTS

We gratefully acknowledge Joe Brunson, Sherri L. Hilligoss, and Don B. McClure for assistance with cell culture for APC expression. We thank Li Li for technical help in animal studies. A. Gupta and B. Gerlitz contributed equally to this work.

DISCLOSURES

The authors disclose that they are employed by Lilly Research Laboratories, a division of Eli Lilly & Co, which produces recombinant human APC for treatment of severe sepsis.

REFERENCES

1. Schrier RW, Wang W, Poole B, Mitra A: Acute renal failure: Definitions, diagnosis, pathogenesis, and therapy. *J Clin Invest* 114: 5–14, 2004
2. Langenberg C, Bellomo R, May C, Wan L, Egi M, Morgera S: Renal blood flow in sepsis. *Crit Care* 9: R363–F374, 2005
3. Chertow GM, Burdick E, Honour M, Bonventre JV, Bates DW: Acute kidney injury, mortality, length of stay, and costs in hospitalized patients. *J Am Soc Nephrol* 16: 3365–3370, 2005
4. Ronco C, Kellum JA, Bellomo R, House AA: Potential interventions in sepsis-related acute kidney injury. *Clin J Am Soc Nephrol* 3: 531–544, 2008
5. Rangel-Frausto MS, Pittet D, Costigan M, Hwang T, Davis CS, Wenzel RP: The natural history of the systemic inflammatory response syndrome (SIRS). A prospective study. *JAMA* 273: 117–123, 1995
6. Riedemann NC, Guo RF, Ward PA: The enigma of sepsis. *J Clin Invest* 112: 460–467, 2003
7. Vincent J, Bota D, De Backer D: Epidemiology and outcome in renal failure. *Int J Artif Organs* 27: 1013–1018, 2004
8. Schrier RW, Wang W: Acute renal failure and sepsis. *N Engl J Med* 351: 159–169, 2004
9. Heuer JG, Sharma GR, Gerlitz B, Zhang T, Bailey DL, Ding C, Berg DT, Perkins D, Stephens EJ, Holmes KC, Grubbs RL, Fynboe KA, Chen YF, Grinnell B, Jakubowski JA: Evaluation of protein C and other biomarkers as predictors of mortality in a rat cecal ligation and puncture model of sepsis. *Crit Care Med* 32: 1570–1578, 2004
10. Macias WL, Nelson DR: Severe protein C deficiency predicts early death in severe sepsis. *Crit Care Med* 32: S223–S228, 2004
11. Gupta A, Berg DT, Gerlitz B, Sharma GR, Syed S, Richardson MA, Sandusky G, Heuer JG, Galbreath EJ, Grinnell BW: Role of protein C in renal dysfunction after polymicrobial sepsis. *J Am Soc Nephrol* 18: 860–867, 2007
12. Gupta A, Rhodes GJ, Berg DT, Gerlitz B, Molitoris BA, Grinnell BW: Activated protein C ameliorates LPS-induced acute kidney injury and downregulates renal INOS and angiotensin 2. *Am J Physiol Renal Physiol* 293: F245–F254, 2007
13. Bernard GR, Vincent JL, Laterre PF, LaRosa SP, Dhainaut JF, Lopez-Rodriguez A, Steingrub JS, Garber GE, Helterbrand JD, Ely EW, Fisher, CJ Jr: Efficacy and safety of recombinant human activated protein C for severe sepsis. *N Engl J Med* 344: 699–709, 2001
14. Mizutani A, Okajima K, Uchiba M, Noguchi T: Activated protein C reduces ischemia/reperfusion-induced renal injury in rats by inhibiting leukocyte activation. *Blood* 95: 3781–3787, 2000
15. Murakami K, Okajima K, Uchiba M, Johno M, Nakagaki T, Okabe H, Takatsuki K: Activated protein C prevents LPS-induced pulmonary vascular injury by inhibiting cytokine production. *Am J Physiol* 272: L197–L202, 1997
16. Esmon CT: The protein C pathway. *Chest* 124: 26S–32S, 2003
17. Mosnier LO, Yang XV, Griffin JH: Activated protein C mutant with minimal anticoagulant activity, normal cytoprotective activity and preservation of TAFI-dependent cytoprotective functions. *J Biol Chem* 282: 33022–33033, 2007
18. Mosnier LO, Griffin JH: Inhibition of staurosporine-induced apoptosis of endothelial cells by activated protein C requires protease-activated receptor-1 and endothelial cell protein C receptor. *Biochem J* 373: 65–70, 2003
19. Joyce DE, Gelbert L, Ciaccia A, DeHoff B, Grinnell BW: Gene expression profile of antithrombotic protein c defines new mechanisms modulating inflammation and apoptosis. *J Biol Chem* 276: 11199–11203, 2001
20. Mosnier LO, Zlokovic BV, Griffin JH: The cytoprotective protein C pathway. *Blood* 109: 3161–3172, 2007
21. O'Brien L, Richardson M, Mehrbod S, Berg D, Gerlitz B, Gupta A, Grinnell B: Activated protein C decreases tumor necrosis factor related apoptosis-inducing ligand by an EPCR- independent mechanism involving Egr-1/Erk-1/2 activation. *Arterioscler Thromb Vasc Biol* 27: 2634–2641, 2007
22. Finigan JH, Dudek SM, Singleton PA, Chiang ET, Jacobson JR, Camp SM, Ye SQ, Garcia JG: Activated protein C mediates novel lung endothelial barrier enhancement: Role of sphingosine 1-phosphate receptor transactivation. *J Biol Chem* 280: 17286–17293, 2005
23. Feistritzer C, Riewald M: Endothelial barrier protection by activated protein C through PAR1-dependent sphingosine 1-phosphate receptor-1 crossactivation. *Blood* 105: 3178–3184, 2005
24. Choi G, Hofstra JJ, Roelofs JJ, Florquin S, Bresser P, Levi M, van der Poll T, Schultz MJ: Recombinant human activated protein C inhibits local and systemic activation of coagulation without influencing inflammation during *Pseudomonas aeruginosa* pneumonia in rats. *Crit Care Med* 35: 1362–1368, 2007
25. Grinnell B, Joyce DE: Recombinant human activated protein C: A system modulator of vascular function for treatment of severe sepsis. *Crit Care Med* 29: S53–S61, 2001
26. Dahlback B: Blood coagulation. *Lancet* 355: 1627–1632, 2000
27. Cheng T, Liu D, Griffin JH, Fernandez JA, Castellino F, Rosen ED, Fukudome K, Zlokovic BV: Activated protein C blocks p53-mediated apoptosis in ischemic human brain endothelium and is neuroprotective. *Nat Med* 9: 338–342, 2003
28. Kerschen E, Fernandez J, Cooley B, Yang X, Sood R, Mosnier L, Castellino F, Mackman N, Griffin J, Weiler H: Endotoxemia and sepsis mortality reduction by non-anticoagulant activated protein C. *J Exp Med* 204: 2439–2448, 2007
29. Esmon CT: Is APC activation of endothelial cell PAR1 important in severe sepsis?: No. *J Thromb Haemost* 3: 1910–1911, 2005
30. Gupta A, Berg DT, Gerlitz B, Richardson MA, Galbreath E, Syed S, Sharma AC, Lowry SF, Grinnell BW: Activated protein C suppresses adrenomedullin and ameliorates lipopolysaccharide-induced hypotension. *Shock* 28: 468–476, 2007
31. Glasscock NL, Gerlitz B, Cooper ST, Grinnell BW, Church FC: Basic residues in the 37-loop of activated protein C modulate inhibition by protein C inhibitor but not by alpha(1)-antitrypsin. *Biochim Biophys Acta* 1647: 106–117, 2003
32. Mosnier LO, Gale AJ, Yegneswaran S, Griffin JH: Activated protein C variants with normal cytoprotective but reduced anticoagulant activity. *Blood* 104: 1740–1744, 2004
33. Isobe H, Okajima K, Uchiba M, Mizutani A, Harada N, Nagasaki A, Okabe K: Activated protein C prevents endotoxin-induced hypotension in rats by inhibiting excessive production of nitric oxide. *Circulation* 104: 1171–1175, 2001
34. Ruf W: Is APC activation of endothelial cell PAR1 important in severe sepsis?: Yes. *J Thromb Haemost* 3: 1912–1914, 2005
35. Naldini A, Carney D, Bocci V, Klimpel K, Asuncion M, Soares L, Klimpel G: Thrombin enhances T cell proliferative responses and cytokine production. *Cell Immunol* 147: 367–377, 1993
36. Shin H, Kitajima I, Nakajima T, Shao Q, Tokioka T, Takasaki I, Hanyu N,

Kubo T, Maruyama I: Thrombin receptor mediated signals induce expressions of interleukin 6 and granulocyte colony stimulating factor via NF-kappa B activation in synovial fibroblasts. *Ann Rheum Dis* 58: 55–60, 1999
37. Fan Y, Zhang W, Mulholland M: Thrombin and PAR-1-AP increase proinflammatory cytokine expression in C6 cells. *J Surg Res* 129: 196–201, 2005
38. Martínez-Sales V, Vila V, Ferrando M, Reganon E: Atorvastatin neutralizes the up-regulation of thrombospondin-1 induced by thrombin in human umbilical vein endothelial cells. *Endothelium* 14: 233–238, 2007
39. Lameire N, Van Biesen W, Vanholder R: Acute renal failure. *Lancet* 365: 417–430, 2005
40. Parikh CR, Abraham E, Ancukiewicz M, Edelstein CL: Urine IL-18 is an early diagnostic marker for acute kidney injury and predicts mortality in the intensive care unit. *J Am Soc Nephrol* 16: 3046–3052, 2005
41. Chin A, Vergnolle N, MacNaughton W, Wallace J, Hollenberg M, Buret A: Proteinase-activated receptor 1 activation induces epithelial apoptosis and increases intestinal permeability. *Proc Natl Acad Sci U S A* 100: 11104–11109, 2003
42. Lopez J, Salido G, Gómez-Arteta E, Rosado J, Pariente J: Thrombin induces apoptotic events through the generation of reactive oxygen species in human platelets. *J Thromb Haemost* 5: 1283–1291, 2007
43. Suzuki T, Moraes T, Vachon E, Ginzberg H, Huang T, Matthay M, Hollenberg M, Marshall J, McCulloch C, Abreu M, Chow C, Downey, G: Proteinase-activated receptor-1 mediates elastase-induced apoptosis of human lung epithelial cells. *Am J Respir Cell Mol Biol* 33: 231–247, 2005
44. Riewald M, Petrovan RJ, Donner A, Mueller BM, Ruf W: Activation of endothelial cell protease activated receptor 1 by the protein C pathway. *Science* 296: 1880–1882, 2002
45. Dear JW, Yasuda H, Hu X, Hieny S, Yuen PS, Hewitt SM, Sher A, Star RA: Sepsis-induced organ failure is mediated by different pathways in the kidney and liver: Acute renal failure is dependent on MyD88 but not renal cell apoptosis. *Kidney Int* 69: 832–836, 2006
46. Molitoris BA, Sutton TA: Endothelial injury and dysfunction: Role in the extension phase of acute renal failure. *Kidney Int* 66: 496–499, 2004
47. Weber JR, Angstwurm K, Rosenkranz T, Lindauer U, Freyer D, Burger W, Busch C, Einhaupl KM, Dirnagl U: Heparin inhibits leukocyte rolling in pial vessels and attenuates inflammatory changes in a rat model of experimental bacterial meningitis. *J Cereb Blood Flow Metab* 17: 1221–1229, 1997
48. Taylor FB Jr, Chang AC, Peer GT, Mather T, Blick K, Catlett R, Lockhart MS, Esmon CT: DEGR-factor Xa blocks disseminated intravascular coagulation initiated by *Escherichia coli* without preventing shock or organ damage. *Blood* 78: 364–368, 1991
49. Abraham E, Reinhart K, Opal S, Demeyer I, Doig C, Rodriguez AL, Beale R, Svoboda P, Laterre PF, Simon S, Light B, Spapen H, Stone J, Seibert A, Peckelsen C, De Deyne C, Postier R, Pettila V, Artigas A, Percell SR, Shu V, Zwingelstein C, Tobias J, Poole L, Stolzenbach JC, Creasey AA: Efficacy and safety of tifacogin (recombinant tissue factor pathway inhibitor) in severe sepsis: A randomized controlled trial. *JAMA* 290: 238–247, 2003
50. Warren BL, Eid A, Singer P, Pillay SS, Carl P, Novak I, Chalupa P, Atherstone A, Penzes I, Kubler A, Knaub S, Keinecke HO, Heinrichs H, Schindel F, Juers M, Bone RC, Opal SM: Caring for the critically ill patient. High-dose antithrombin III in severe sepsis: A randomized controlled trial. *JAMA* 286: 1869–1878, 2001
51. Laemmli U: Cleavage of structural proteins during the assembly of the head of bacteriophage T4. *Nature* 227: 680–685, 1970
52. Gerlitz B, Hassell T, Vlahos C, Parkinson JF, Bang NU, Grinnell BW: Identification of the predominant glycosaminoglycan-attachment site in soluble recombinant human thrombomodulin: Potential regulation of functionality by glycosyltransferase competition for serine 474. *Biochem J* 295: 131–140, 1993
53. Fukudome K, Kurosawa S, Stearns-Kurosawa D, He X, Rezaie A, Esmon C: The endothelial cell protein C receptor. Cell surface expression and direct ligand binding by the soluble receptor. *J Biol Chem* 271: 17491–17498, 1996
54. Sandusky G, Berg DT, Richardson MA, Myers L, Grinnell BW: Modulation of thrombomodulin-dependent activation of human protein C through differential expression of endothelial Smads. *J Biol Chem* 277: 49815–49819, 2002
55. Bentley MD, Lerman LO, Hoffman EA, Fiksen-Olsen MJ, Ritman EL, Romero JC: Measurement of renal perfusion and blood flow with fast computed tomography. *Circ Res* 74: 945–951, 1994
56. Hillman BJ, Lee SM, Tracey P, Swindell W, Long DM: CT determination of renal and hepatic microvascular volumes in experimental acute renal failure. *Invest Radiol* 17: 41–45, 1982
57. Kan Z, Phongkitkarun S, Kobayashi S, Tang Y, Ellis LM, Lee TY, Charnsangavej C: Functional CT for quantifying tumor perfusion in antiangiogenic therapy in a rat model. *Radiology* 237: 151–158, 2005
58. Young LS, Regan MC, Barry MK, Geraghty JG, Fitzpatrick JM: Methods of renal blood flow measurement. *Urol Res* 24: 149–160, 1996
59. Sutton T, Fisher C, Molitoris B: Microvascular endothelial injury and dysfunction during ischemic acute renal failure. *Kidney Int* 62: 1539–1549, 2002
60. Friedewald J, Rabb H: Inflammatory cells in ischemic acute renal failure. *Kidney Int* 66: 486–491, 2004

Supplemental information for this article is available online at http://www.jasn.org/.